Two-Photon Blockade in an Atom-Driven Cavity QED System

Christoph Hamsen,* Karl Nicolas Tolazzi, Tatjana Wilk, and Gerhard Rempe
Max-Planck-Institut für Quantenoptik, Hans-Kopfermann-Straße 1, 85748 Garching, Germany
(Received 4 August 2016; published 31 March 2017)

Photon blockade is a dynamical quantum-nonlinear effect in driven systems with an anharmonic energy ladder. For a single atom strongly coupled to an optical cavity, we show that atom driving gives a decisively larger optical nonlinearity than cavity driving. This enhances single-photon blockade and allows for the implementation of two-photon blockade where the absorption of two photons suppresses the absorption of further photons. As a signature, we report on three-photon antibunching with simultaneous two-photon bunching observed in the light emitted from the cavity. Our experiment constitutes a significant step towards multiphoton quantum-nonlinear optics.

DOI: 10.1103/PhysRevLett.118.133604

An open driven quantum system exhibits fluctuations that reflect its walk through Hilbert space. Blocking parts of the Hilbert space can reduce these fluctuations and stabilize the output. For discrete variables like particle number, blockade occurs for sufficiently strong interaction between the involved quanta. Examples include the Coulomb force for electrons or the effective interaction between photons in an optically nonlinear medium. The latter has been used to realize single-photon blockade [1], where $n = 1$ photon blocks further photons so that they are emitted one by one [2–8]. The challenge now is to scale the blockade to $n > 1$ photons [9–11] and produce a photon stream with at most n photons. Such quantum scissors could lead to novel applications in multiphoton quantum-nonlinear optics like an n-photon source [12].

An ideal platform for the implementation of an optical n-photon blockade is cavity quantum electrodynamics (QED), which strongly couples a single two-level atom, perfectly blockaded at one photon, to a cavity that is completely unblocked. Both subsystems alone fail to show multiphoton blockade: the cavity needs the nonlinearity introduced by the atom, and the atom needs access to the larger Hilbert space provided by the cavity. Only the combined system with its anharmonic energy-level structure provides the necessary photon-number dependent nonlinearity. Nevertheless, realization of multiphoton blockade is challenging due to the limited atom-cavity coupling strength that has so far been obtained [13–15]. Although strategies have been proposed to improve the blockade by extension to a three- or four-level atom involving electromagnetically induced transparency [16,17] or Raman scattering [18,19], multiphoton blockade has not been observed in optical systems. Its demonstration in circuit QED seems pending, too, although well-resolved multiphoton transitions have been investigated [20–22].

This Letter reports on the first experimental observation of two-photon blockade with a strongly coupled atom-cavity system. Specifically, we demonstrate an increased excitation of the system's second energy manifold in combination with a suppressed excitation of the third and higher manifolds. As a signature, the light emitted from the cavity exhibits a pronounced three-photon antibunching with simultaneous two-photon bunching when driving the system close to a two-photon resonance [23]. We show that two-photon blockade exists only for excitation of the system via the atom, while cavity driving at this frequency yields strong bunching of second- and third-order photon correlations. The novel dependence on the excitation path can be understood intuitively as a consequence of bosonic enhancement of photons when driving the cavity, an effect which facilitates climbing up the ladder of dressed atom-cavity states. The atom, in contrast, can absorb only one photon at a time and thus makes the unwanted climbing more difficult. We therefore claim that in order to exploit the full optical nonlinearity of the system for the realization of, e.g., an n-photon absorber or an n-photon emitter, it is more favorable to drive the atom instead of the cavity.

The dependence of the nonlinear behavior on the driven component can be expressed quantitatively by calculating the transition strengths in the dressed state basis. The driven atom-cavity system as depicted in Fig. 1(a) is well described by the Jaynes-Cummings Hamiltonian [35] plus a driving term H_d, here in rotating-wave approximation:

$$H = \hbar\Delta_a\hat{\sigma}^\dagger\hat{\sigma} + \hbar\Delta_c\hat{a}^\dagger\hat{a} + \hbar g(\hat{a}^\dagger\hat{\sigma} + \hat{\sigma}^\dagger\hat{a}) + H_d, \quad (1)$$

where $\Delta_a = \omega_d - \omega_a$ ($\Delta_c = \omega_d - \omega_c$) is the atom (cavity) detuning with respect to the driving frequency ω_d, $\hat{\sigma}^\dagger$ ($\hat{\sigma}$) is the atomic raising (lowering) operator, and $\hat{a}^\dagger$ ($\hat{a}$) is the photon creation (annihilation) operator with $\hat{n} = \hat{a}^\dagger\hat{a}$ being the photon number operator. While the first two terms in Eq. (1) correspond to the bare energy eigenstates of emitter and resonator, the third term describes their interaction with coupling strength g. This yields energy eigenstates that form an anharmonic ladder of doublets

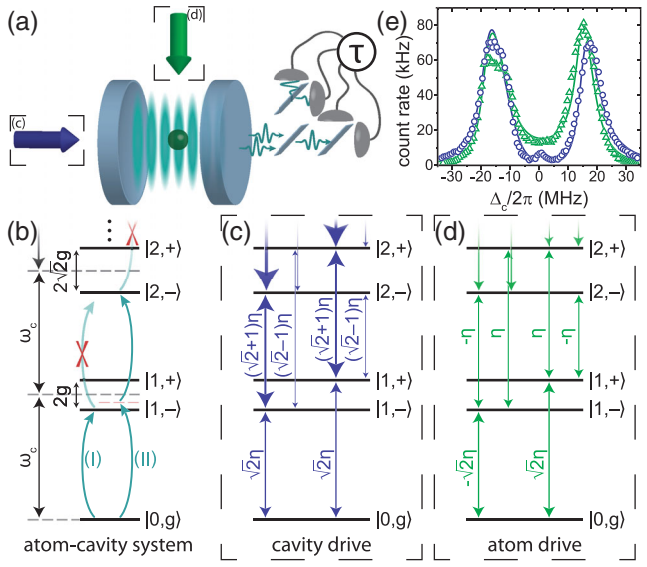

FIG. 1. Sketch of the experimental setup and physical system. As depicted in (a), a single atom is trapped at the antinode of an intracavity light field. The anharmonic energy-ladder system (b) can either be excited via a cavity [blue, effective driving strengths see (c)] or atom drive [green, effective driving strengths see (d)]. The resulting cavity field is then monitored via an extended Hanbury Brown–Twiss detection setup. Spectra for driving the cavity (blue circles) or the atom (green triangles) are shown in (e). The thick colored lines are fits of a model considering residual thermal excitation and possible remnants of the empty cavity [23]. Symbols: cavity frequency ω_c, coupling strength g, driving strength η, probe-cavity detuning Δ_c.

$[|n,\pm\rangle = (|n,g\rangle \pm |n-1,e\rangle)/\sqrt{2}]$ split by $2\sqrt{n}g$, referred to as dressed states [Fig. 1(b)]. Single- and two-photon blockade are then expected for resonant one- and two-photon excitation of the first (I) and second (II) manifold, respectively.

The last term in Eq. (1) describes the excitation via the driving field. The energy structure remains unaffected as long as the drive strength is much smaller than g and does not exceed the atomic polarization decay rate γ and cavity-field decay rate κ [36]. However, the corresponding excitation strengths between different manifolds differ whether the cavity is driven, $H_d = \hbar\eta_c(\hat{a} + \hat{a}^\dagger)$, or the atom, $H_d = \hbar\eta_a(\hat{\sigma} + \hat{\sigma}^\dagger)$ [37]. Here, η_c (η_a) is the strength of the cavity (atom) drive. Both strengths are expressed for the bare eigenstates of the system without atom-cavity interaction. Reformulation in the dressed state basis of the coupled system ($|n,\pm\rangle$) yields effective strengths $\tilde{\eta}_c/2$ or $\tilde{\eta}_a/2$ for the cavity or atom drive, respectively. For the transition from the ground state to the first manifold, $|0,g\rangle \to |1,\pm\rangle$, these are $\tilde{\eta}_a = \pm\sqrt{2}\eta_a$ and $\tilde{\eta}_c = \sqrt{2}\eta_c$. For the transition from the nth to the $(n+1)$th manifold, and in the case of cavity driving, bosonic bunching causes symmetry conserving transitions ($|n,\pm\rangle \to |n+1,\pm\rangle$) to be strongly enhanced by $\tilde{\eta}_c = (\sqrt{n+1} + \sqrt{n})\eta_c$, whereas those that change symmetry ($|n,\pm\rangle \to |n+1,\mp\rangle$) are suppressed, $\tilde{\eta}_c = (\sqrt{n+1} - \sqrt{n})\eta_c$ [Fig. 1(c)]. For an atom drive, all transitions have equal strengths, with the sign being that of the upper state, $\tilde{\eta}_a = \pm\eta_a$ [Fig. 1(d)].

As a consequence, resonant driving of the nth manifold via the cavity reduces the suppression of higher excitations since the corresponding transition strengths increase. In contrast, the transition strengths remain constant when driving the atom. As will be shown in the following, the resulting stronger suppression of higher rungs for atom excitation manifests itself in an improved purity of single-photon emission on the first manifold and enables two-photon blockade on the second manifold.

In our system, a single ^{87}Rb atom ($\gamma/2\pi = 3.0$ MHz) is loaded into the center of a high-finesse Fabry-Perot resonator with length 200 μm and a field decay rate $\kappa/2\pi = 2.0$ MHz [23]. Two blue- and one red-detuned standing-wave optical dipole traps form a three-dimensional lattice that confines the atom to an antinode of the cavity field [38]. The dynamical Stark shift, mainly caused by the red-detuned 800 nm trap, reduces the atom-cavity detuning, $\Delta_{ac}/2\pi = (\omega_a - \omega_c)/2\pi = -15.2$ MHz, to the $F = 2 \leftrightarrow F' = 3$ transition of the D_2 line at 780 nm to only a few MHz. We use the transition with the largest dipole matrix element between Zeeman states $m_F = +2 \leftrightarrow m_F' = +3$. Here, an atom-cavity coupling strength of $g/2\pi = 20$ MHz puts the experiment well into the strong-coupling regime of cavity QED, $g \gg (\kappa, \gamma)$.

As long as the atom is trapped (typically 5 s), we repeat our measurement sequence with a rate of 2 kHz. This sequence consists of a cooling interval, state preparation of the $F = 2$, $m_F = +2$ state, and a probe interval during which we apply the respective probe (alternating from sequence to sequence) at the desired frequency and record the transmitted signal on 4 single-photon detectors with a timing resolution of 1 ns. The power is chosen such that we remain in the weak driving regime, $\eta_{a,c} \leq (\kappa, \gamma)$.

Spectra for atom and cavity driving are depicted in Fig. 1(e). In both cases, the distinct splitting of the normal modes reflects the strong coupling of the system. We deduce an experimental coupling constant of $g/2\pi = 16.38(4)$ MHz. The stronger drop of transmission in case of cavity driving results from the atomic antiresonance caused by destructive interference when exciting the cavity [39]. This also slightly increases the observed normal mode splitting.

To demonstrate single-photon blockade and its dependence on the driven component, we start by exciting the system close to the first manifold. The measured second-order photon correlation function $g^{(2)}(\tau) = \langle \hat{n} \cdot \hat{n}(\tau) \rangle / \langle \hat{n} \rangle^2$ (normal and time ordered) for atom driving ($\eta_a/2\pi \approx 0.55$ MHz) is shown in Fig. 2(a) with the corresponding theory as an inset. A strong sub-Poissonian antibunching with a $g^{(2)}(0) = 0.16(1)$ and a rising slope indicate emission of single light quanta due to a strong

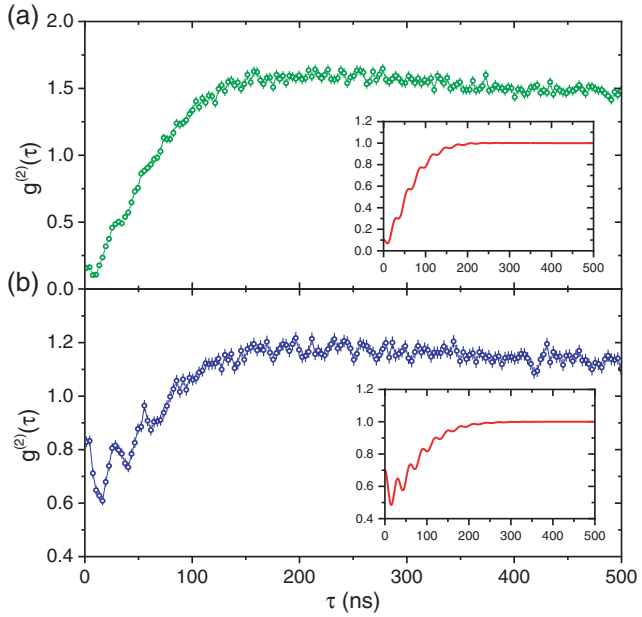

FIG. 2. The second-order photon correlation function for (a) atom and (b) cavity excitation of the first manifold at $\Delta_c/2\pi =$ 18 MHz with a binning of 3 ns reveals single-photon blockade. Here, and in Figs. 3–5, error bars are statistical, indicating 1 standard deviation, and theory (insets) is calculated via numerical solution of the master equation [23]. Theory is shown for qualitative comparison, deviations to experimental results stem from atomic motion and position distribution of atoms within the cavity mode.

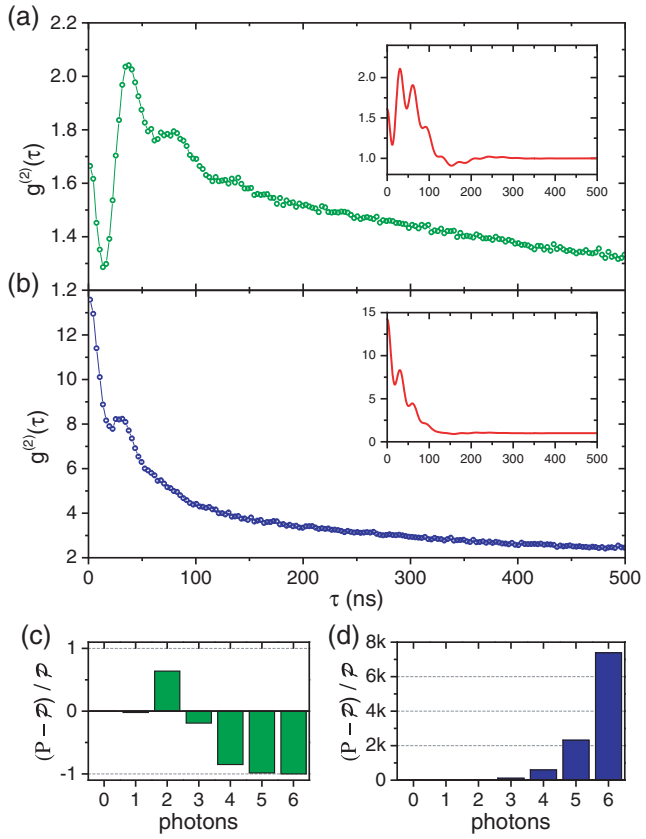

FIG. 3. Close to the second manifold at $\Delta_c/2\pi = 9$ MHz, photon correlations with 3 ns binning for (a) atom and (b) cavity driving show bunching. Insets depict the corresponding theory, which we add for qualitative comparison. The relative deviations of the simulated photon distribution to a Poisson distribution of the same mean photon number indicate two-photon blockade for atom (c) but not cavity (d) excitation. In (d), the ordinate is scaled by a factor of $k = 1000$.

blockade of multiple excitations [compare Fig. 1(b,I)]. We observe a small and rapid oscillation at approximately twice the coupling rate g known as vacuum Rabi oscillation [40]. It originates from the coherent energy exchange between atom and cavity. We estimate the coupling rate from the second oscillation maximum at 31.5(15) ns to be 15.9(8) MHz which is in good agreement with the fitted value from the spectrum. The nonclassical behavior disappears on a time scale determined by the decay rate of the excited dressed state $[(\kappa+\gamma)/2]^{-1} \approx 64$ ns. The classical value, achieved for large correlation times, deviates from 1 due to motion and residual displacement from the cavity-mode center [23,40].

Excitation of the cavity ($\eta_c/2\pi \approx 0.55$ MHz) on the first manifold is depicted in Fig. 2(b) and yields qualitatively the same behavior. However, the value $g^{(2)}(0) = 0.83(2)$ is much larger, and stronger vacuum Rabi oscillations indicate significant excitation of higher manifolds. In accordance with theory, atom driving does exhibit a far stronger photon blockade effect despite the same energy-level structure.

In order to investigate two-photon blockade, we tune the drives close to the second manifold [compare Fig. 1(b,II)] and increase their strengths to $\eta_a/2\pi \approx$ 1.6 MHz and $\eta_c/2\pi \approx 1.1$ MHz, approaching the cavity decay rate to allow for significant population of higher states without yet affecting the level structure. As shown in Figs. 3(a) and 3(b), this yields super-Poissonian emission in both cases since $g^{(2)}(0) > 1$ which is indicative of higher photon numbers. While cavity excitation shows the expected bunching behavior [41], the observed dynamics for atom driving is more complex. The interplay between conflicting mechanisms, a two-photon resonance on one hand, and an emitter that can only absorb one excitation at a time on the other hand, leads to a novel photon-concatenation effect. Since the rate of coherent energy exchange between atom and cavity exceeds the spontaneous decay rate of the system, higher manifolds are populated in stepwise excitation via the emitter. As a consequence, we observe that the second-order correlation function peaks 37.5(15) ns after the trigger photon which indicates that the coupling rate rather than the lifetime determines the probability for detection of a second photon, in contrast to the first-manifold dynamics described above. As $g^{(2)}(\tau) > g^{(2)}(0)$, this behavior violates the Cauchy-Schwarz inequality and is thus quantum in nature [42,43].

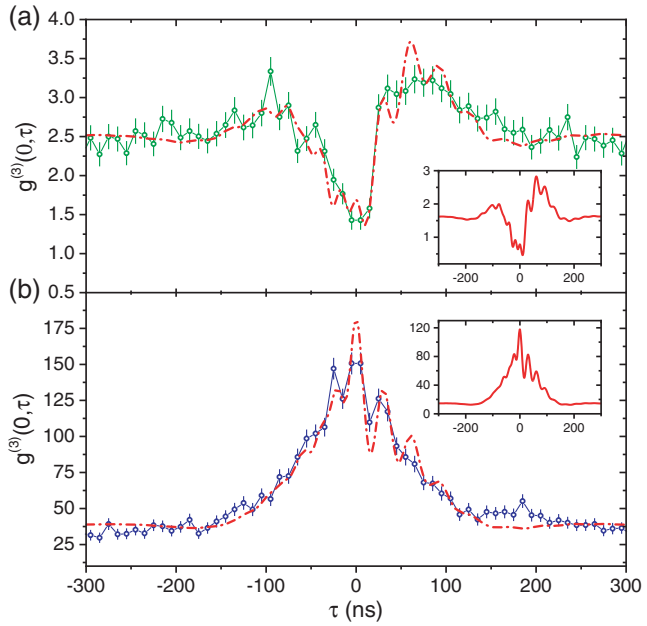

FIG. 4. The third-order photon correlation function $g^{(3)}(0,\tau)$ is depicted for (a) atom and (b) cavity excitation close to the second manifold with a binning of 10 ns. For qualitative comparison, the theory for the same parameters (inset) has been scaled and shifted to fit experimental data (dash dotted red lines).

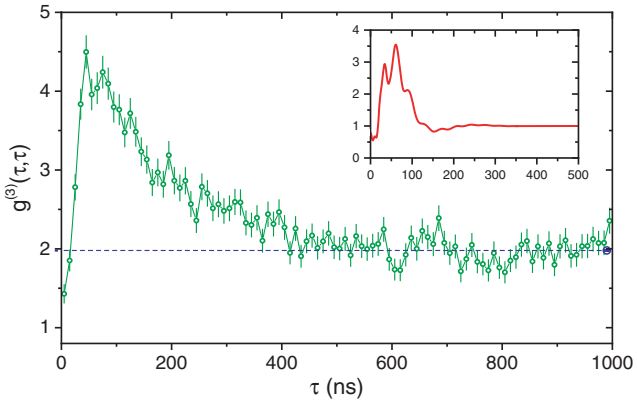

FIG. 5. The third-order photon correlation function $g^{(3)}(\tau,\tau)$ for atom driving close to the second manifold with a binning of 10 ns is depicted. The inset shows the result expected by theory. The blue empty marker and dashed line indicate the long-time average for 1 to 4 μs (after the correlation has settled) which is clearly above $g^{(3)}(0,0)$.

While Figs. 3(a) and 3(b) indicate multiphoton emission, a two-photon blockade furthermore requires suppression of excitation to even higher manifolds. To illustrate this, we calculate the full photon-number distribution $P(n)$ and compare this to a Poisson distribution $\mathcal{P}(n)$ of the same mean photon number as depicted in Figs. 3(c) and 3(d). For cavity driving, the relative population grows with the excitation number as expected due to bosonic enhancement. In case of atom excitation, we see enhanced two-photon emission while higher Fock states are increasingly suppressed. The latter condition can be understood as truncation of the Hilbert space and indicates two-photon blockade that for our parameters is only visible for atom driving.

For demonstrating two-photon blockade, we evaluate the third-order photon correlation $g^{(3)}(\tau_1,\tau_2) = \langle \hat{n}\cdot\hat{n}(\tau_1)\cdot\hat{n}(\tau_1+\tau_2)\rangle/\langle\hat{n}\rangle^3$ (normal and time ordered). Here, we discuss two specific cases. We start with the dynamically interesting case of $(\tau_1,\tau_2) = (0,\tau)$ where the third-order correlation yields information on the conditional evolution of $\langle\hat{n}\rangle$ ($\langle\hat{n}^2\rangle$), i.e., the dynamics on the first (second) manifold for positive (negative) τ [44]. This is depicted in Figs. 4(a) and 4(b) for atom and cavity driving, respectively. We find good qualitative agreement with theory that for comparison has been shifted and scaled to again compensate for effects due to atomic motion and residual position distribution within the cavity. Note that for large τ one cannot expect $g^{(3)}(0,\tau)$ to approach 1, but the value of $g^{(2)}(0)g^{(2)}(\tau)$ since two of the photons are correlated for any τ [45]. The asymmetry and different oscillation frequencies for positive and negative times reflect the coherent evolution on the first and second manifold at frequency $2g$ and $2\sqrt{2}g$, respectively [44]. Most striking is that atom and cavity excitation exhibit very different behavior towards zero time delay: We observe antibunching when driving the atom in contrast to a strong bunching for cavity excitation. As a consequence, higher photon numbers are suppressed (enhanced) when exciting the atom (cavity) into the second manifold.

To prove suppression of three-photon emission, we evaluate $g^{(3)}(\tau,\tau)$ for atom driving as shown in Fig. 5. For time intervals exceeding the time scale of the internal coherence, $\tau \gg 2/(\kappa+\gamma)$, $g^{(3)}(\tau,\tau)$ is proportional to the probability of detecting three uncorrelated photons. In contrast to theory, $g^{(3)}(0,0) = 1.43(12)$ is above 1, the value expected for a Poissonian light field. However, we do significantly underpass the long-term averaged value of 1.98(1) that serves as a reference for uncorrelated photons. This value is above 1 due to technical fluctuations that shift $g^{(3)}(\tau,\tau)$ to higher values [23]. To confirm this, we calculate our photon distribution $P(n)$ from the number of photons per measurement interval, averaged over many realizations, and deduce a value of $g^{(3)}(0,0) = [\sum_n n(n-1)(n-2)P(n)]/[\sum_n nP(n)]^3 = 1.99$ for uncorrelated photons. This value agrees very well with the long-time averaged $g^{(3)}(\tau,\tau)$ and proves an increased variance of the field, likely due to residual atom motion and a distribution of positions with respect to the cavity mode and atom drive [23]. We conclude that the $g^{(3)}(\tau,\tau)$, therefore, demonstrates a two-photon blockade where the probability of detecting more than two photons for zero time delay is reduced.

In conclusion, we have shown that driving the quantum emitter instead of the resonator improves the nonlinear response of the strongly coupled system. This allows us to

demonstrate both single- and two-photon blockade. Future experiments could explore the extension of the blockade mechanism to even higher photon numbers. For example, simulations indicate that three-photon blockade seems feasible with our system. As blockade truncates the high end of the photon-number distribution, any additional reduction of the low end [5,41] may enable carving of various nonclassical photon states like those containing n photons. Direct production of n-photon states has also been proposed for strong atom driving, $\eta_a \gg g$, with the cavity tuned as to selectively enhance a specific n-photon transition between dressed atom-laser states [46]. Selective population of higher-energetic atom-cavity states might be possible by stepwise excitation of the symmetry-changing transitions ($|n, \pm\rangle \rightarrow |n+1, \mp\rangle$). When exciting the atom instead of the cavity, these transitions exhibit larger and thus more favorable strengths [20]. Finally, driving atom and cavity simultaneously might enable a quantum interference induced photon blockade where single-photon emission results from destructive interference between different transition paths [47].

We thank H. Chibani, B. Dayan, A. González-Tudela, and S. Dürr for discussions. P. A. Altin, M. Bernard-Schwarz, and A. C. Eckl contributed to the implementation of the experiment. C. H. acknowledges support from the Deutsche Forschungsgemeinschaft via the excellence cluster Nanosystems Initiative Munich (NIM).

*Christoph.Hamsen@mpq.mpg.de

[1] A. Imamoglu, H. Schmidt, G. Woods, and M. Deutsch, Phys. Rev. Lett. **79**, 1467 (1997).
[2] H. J. Kimble, M. Dagenais, and L. Mandel, Phys. Rev. Lett. **39**, 691 (1977).
[3] K. M. Birnbaum, A. Boca, R. Miller, A. D. Boozer, T. E. Northup, and H. J. Kimble, Nature (London) **436**, 87 (2005).
[4] B. Dayan, A. S. Parkins, T. Aoki, E. P. Ostby, K. J. Vahala, and H. J. Kimble, Science **319**, 1062 (2008).
[5] A. Faraon, I. Fushman, D. Englund, N. Stoltz, P. Petroff, and J. Vučković, Nat. Phys. **4**, 859 (2008).
[6] A. Reinhard, T. Volz, M. Winger, A. Badolato, K. J. Hennessy, E. L. Hu, and A. Imamoglu, Nat. Photonics **6**, 93 (2011).
[7] C. Lang, D. Bozyigit, C. Eichler, L. Steffen, J. M. Fink, A. A. Abdumalikov, M. Baur, S. Filipp, M. P. da Silva, A. Blais, and A. Wallraff, Phys. Rev. Lett. **106**, 243601 (2011).
[8] A. J. Hoffman, S. J. Srinivasan, S. Schmidt, L. Spietz, J. Aumentado, H. E. Türeci, and A. A. Houck, Phys. Rev. Lett. **107**, 053602 (2011).
[9] S. S. Shamailov, A. S. Parkins, M. J. Collett, and H. J. Carmichael, Opt. Commun. **283**, 766 (2010).
[10] A. Miranowicz, M. Paprzycka, Y.-X. Liu, J. Bajer, and F. Nori, Phys. Rev. A **87**, 023809 (2013).
[11] H. J. Carmichael, Phys. Rev. X **5**, 031028 (2015).
[12] D. E. Chang, V. Vuletić, and M. D. Lukin, Nat. Photonics **8**, 685 (2014).
[13] K. J. Vahala, Nature (London) **424**, 839 (2003).
[14] M. Devoret, S. Girvin, and R. Schoelkopf, Ann. Phys. (Leipzig) **16**, 767 (2007).
[15] I. Schuster, A. Kubanek, A. Fuhrmanek, T. Puppe, P. W. H. Pinkse, K. Murr, and G. Rempe, Nat. Phys. **4**, 382 (2008).
[16] S. Rebic, S. M. Tan, A. S. Parkins, and D. F. Walls, J. Opt. B **1**, 490 (1999).
[17] J. A. Souza, E. Figueroa, H. Chibani, C. J. Villas-Boas, and G. Rempe, Phys. Rev. Lett. **111**, 113602 (2013).
[18] S. Rosenblum, S. Parkins, and B. Dayan, Phys. Rev. A **84**, 033854 (2011).
[19] S. Rosenblum, O. Bechler, I. Shomroni, Y. Lovsky, G. Guendelman, and B. Dayan, Nat. Photonics **10**, 19 (2015).
[20] J. M. Fink, M. Göppl, M. Baur, R. Bianchetti, P. J. Leek, A. Blais, and A. Wallraff, Nature (London) **454**, 315 (2008).
[21] F. Deppe, M. Mariantoni, E. P. Menzel, A. Marx, S. Saito, K. Kakuyanagi, H Tanaka, T. Meno, K. Semba, H. Takayanagi, E. Solano, and R. Gross, Nat. Phys. **4**, 686 (2008).
[22] L. S. Bishop, J. M. Chow, J. Koch, A. A. Houck, M. H. Devoret, E. Thuneberg, S. M. Girvin, and R. J. Schoelkopf, Nat. Phys. **5**, 105 (2009).
[23] See Supplemental Material at http://link.aps.org/supplemental/10.1103/PhysRevLett.118.133604 for more information on the theory of multiphoton blockade, the apparatus and atom trapping, the experimental sequence, the simulation model, and correlations, statistics and fluctuations, which includes Refs. [24–34].
[24] K. M. Birnbaum, A. Boca, R. Miller, A. D. Boozer, T. E. Northup, and H. J. Kimble, arXiv:quant-ph/0507065.
[25] S. Nußmann, K. Murr, M. Hijlkema, B. Weber, A. Kuhn, and G. Rempe, Nat. Phys. **1**, 122 (2005).
[26] K. Murr, J. Phys. B **36**, 2515 (2003).
[27] A. Neuzner, M. Körber, O. Morin, S. Ritter, and G. Rempe, Nat. Photonics **10**, 303 (2016).
[28] P. Maunz, T. Puppe, I. Schuster, N. Syassen, P. W. H. Pinkse, and G. Rempe, Phys. Rev. Lett. **94**, 033002 (2005).
[29] H. J. Carmichael, *An Open Systems Approach to Quantum Optics* (Springer, Berlin, 1993).
[30] C. Gardiner and P. Zoller, *Quantum Noise* (Springer, Berlin, 2004).
[31] J. Johansson, P. Nation, and F. Nori, Comput. Phys. Commun. **184**, 1234 (2013).
[32] F. Diedrich and H. Walther, Phys. Rev. Lett. **58**, 203 (1987).
[33] D. Rotter, M. Mukherjee, F. Dubin, and R. Blatt, New J. Phys. **10**, 043011 (2008).
[34] A. Rundquist, M. Bajcsy, A. Majumdar, T. Sarmiento, K. Fischer, K. G. Lagoudakis, S. Buckley, A. Y. Piggott, and J. Vučković, Phys. Rev. A **90**, 023846 (2014).
[35] E. Jaynes and F. Cummings, Proc. IEEE **51**, 89 (1963).
[36] P. Alsing, D.-S. Guo, and H. J. Carmichael, Phys. Rev. A **45**, 5135 (1992).
[37] P. Alsing and H. J. Carmichael, Quantum Opt. **3**, 13 (1991).
[38] A. Reiserer, C. Nölleke, S. Ritter, and G. Rempe, Phys. Rev. Lett. **110**, 223003 (2013).
[39] C. Sames, H. Chibani, C. Hamsen, P. A. Altin, T. Wilk, and G. Rempe, Phys. Rev. Lett. **112**, 043601 (2014).
[40] G. Rempe, R. J. Thompson, R. J. Brecha, W. D. Lee, and H. J. Kimble, Phys. Rev. Lett. **67**, 1727 (1991).
[41] A. Kubanek, A. Ourjoumtsev, I. Schuster, M. Koch, P. W. H. Pinkse, K. Murr, and G. Rempe, Phys. Rev. Lett. **101**, 203602 (2008).

[42] L. Mandel and E. Wolf, *Optical Coherence and Quantum Optics* (Cambridge University Press, Cambridge, England, 1995).

[43] S. L. Mielke, G. T. Foster, and L. A. Orozco, Phys. Rev. Lett. **80**, 3948 (1998).

[44] M. Koch, C. Sames, M. Balbach, H. Chibani, A. Kubanek, K. Murr, T. Wilk, and G. Rempe, Phys. Rev. Lett. **107**, 023601 (2011).

[45] M. Koch, Ph. D. thesis, Technische Universität München, 2011.

[46] C. S. Muñoz, E. del Valle, A. G. Tudela, K. Müller, S. Lichtmannecker, M. Kaniber, C. Tejedor, J. J. Finley, and F. P. Laussy, Nat. Photonics **8**, 550 (2014).

[47] J. Tang, W. Geng, and X. Xu, Sci. Rep. **5**, 9252 (2015).